Mon. Not. R. Astron. Soc. **342,** 69–78 (2003)

Orbital dynamics of three-dimensional bars – IV. Boxy isophotes in face-on views

P. A. Patsis,[1⋆] Ch. Skokos[1,2] and E. Athanassoula[3]

[1]*Research Centre of Astronomy, Academy of Athens, Anagnostopoulou 14, GR-10673 Athens, Greece*
[2]*Division of Applied Analysis, Department of Mathematics and Centre for Research and Application of Nonlinear Systems (CRANS), University of Patras, GR-26500 Patras, Greece*
[3]*Observatoire de Marseille, 2 Place Le Verrier, F-13248 Marseille Cedex 4, France*

Accepted 2003 February 6. Received 2003 February 4; in original form 2002 August 9

ABSTRACT

We study the conditions that favour boxiness of isodensities in the face-on views of orbital 3D models for barred galaxies. Using orbital weighted profiles we show that boxiness is in general a composite effect that appears when one considers stable orbits belonging to several families of periodic orbits. 3D orbits that are introduced due to vertical instabilities play a crucial role in the face-on profiles and enhance their rectangularity. This happens because at the 4:1 radial resonance region we have several orbits with boxy face-on projections, instead of a few rectangular-like x1 orbits, which, in a fair fraction of the models studied so far, are unstable in this region. Massive bars are characterized by rectangular-like orbits. However, we find that it is the pattern speed that affects the elongation of the boxy feature most, in the sense that fast bars are more elongated than slow ones. Boxiness in intermediate distances between the centre of the model and the end of the bar can be attributed to x1v1 orbits, or to a combination of families related to the radial 3:1 resonance.

Key words: galaxies: evolution – galaxies: kinematics and dynamics – galaxies: structure.

1 INTRODUCTION

Boxy isophotes are a typical feature at the end of the bars of early type (SB0, SBa) barred galaxies seen not far from face-on. Typical examples can be found in Athanassoula et al. (1990) (NGC 936, NGC 4314, NGC 4596), in Buta (1986) (NGC 1433), in Ohta, Hamabe & Wakamatsu (1990) (NGC 2217, NGC 4440, NGC 4643, NGC 4665) and in many other papers. Loosely speaking, the shape of these isophotes is rectangular-like. Their main characteristic is that their small sides, at the largest distance of the isophotes from the galactic centre, are roughly parallel to the bar minor axis (Athanassoula 1984; Athanassoula et al. 1990; Elmegreen 1996). In particular, Athanassoula et al. (1990) use generalized ellipses to fit the isophotes of the bars in a sample of early-type strongly barred galaxies, thus describing quantitatively the result that the shapes of the isophotes are rectangular-like rather than elliptical-like. Fig. 1 is a DSS image of NGC 4314 in *B* and demonstrates a typical case of a galaxy with boxy isophotes at the end of its bar. We observe that the last isophotes of the bar are indeed rectangular-like. Beyond the area of the boxy isophotes starts the spiral structure of this galaxy.

There is a correspondence between the morphology of the boxy isophotes of the early-type barred galaxies and the isodensities encountered in snapshots of several *N*-body models of bars. This was shown for the first time in a simulation that was run specifically for this purpose (Athanassoula et al. 1990, fig. 7). In that paper this correspondence was underlined by measuring the rectangularity in the same way as in the observations. Since then there have been several snapshots in *N*-body simulations reproducing this morphological feature (see e.g. Shaw et al. 1993; Friedli & Benz 1993; Debattista & Sellwood 2000). Recently Athanassoula & Misiriotis (2002) in their *N*-body models describe this feature also quantitatively. We can thus conclude that both observations and numerical models clearly show that boxiness close to the end of the bars is a very frequently encountered phenomenon, and thus it should be related to the standard dynamical behaviour in such systems.

Early calculations of orbits in 2D static potentials have underlined the presence of rectangular-like periodic orbits in the 4:1 resonance region (Athanassoula et al. 1983; Contopoulos 1988; Athanassoula 1992a). They are either orbits of the x1 family on the decreasing part of the characteristic (towards lower x values) in type-2 4:1 resonance gaps,[1] or orbits at the '4:1 branch' beyond the type-1 gap (Contopoulos 1988). These orbits, whenever they exist, support outer boxiness on the face-on views of the models. Their mere presence, however, is not sufficient to explain the observed morphology.

⋆E-mail: ppatsis@cc.uoa.gr

[1] For the nomenclature of the gaps see Contopoulos (1988), or Contopoulos & Grosbøl (1989).

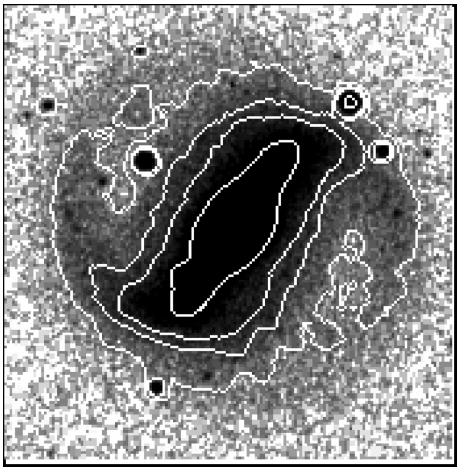

Figure 1. DSS image of NGC 4314 in the *B* band.

Explanations based on the presence of rectangular-like planar 2D x1 orbits suffer from the following problems.

(i) The range of the Jacobi integral[2] over which one finds *stable* rectangular-like x1 orbits (in type-2 gaps) or 4:1 orbits (in type-1 gaps) is in general narrow (Contopoulos & Grosbøl 1989). Furthermore, these orbits develop loops at the four corners, the size of which increases considerably with energy, while the near-horizontal sections of the orbit approach the minor axis (as in fig. 3d in Athanassoula 1992a). This happens for energies only a little larger than the energy at which the orbits become rectangular-like. Orbits with loops cannot easily reproduce the observed boxiness. Thus, we have only a very small energy interval with useful orbits (see fig. 8 in Athanassoula et al. 1990).

(ii) Poincaré sections for an energy value within the small energy interval where rectangular-like orbits are stable show that the size of the stability area is very small (see e.g. fig. 21 in Patsis, Athanassoula & Quillen 1997a). This renders the trapping of many non-periodic orbits around stable boxy periodic orbits rather difficult. It is characteristic that Patsis et al. (1997b) used dynamical spectra in order to trace tiny stability islands of rectangular-like orbits in a 2D Ferrers bar potential.

(iii) In many models the orbital rectangles are not sufficiently elongated. They frequently are rather square-like, even in cases of strong bars (as in fig. 3c in Athanassoula 1992a).

Besides the papers of Contopoulos on non-linear phenomena at the 4:1 resonance region in 2D bars in the 1980s, and the work of Athanassoula and collaborators on the morphology of bar orbits in the early 1990s, where the problem is explicitly stated, not much work has been done on this issue. Nevertheless, from figures of orbits in models of 3D bars (Pfenniger 1984, 1985) one can infer that problems like the squareness of the rectangular-like orbits persist even if one considers also the third dimension of the bars. The morphology of single orbits, however, does not determine the boxiness of the isodensities of a model.

The goal of the present paper is to reconsider the problem of rectangular-like isodensities in the framework of 3D orbital structure models, and, more specifically, to examine the contribution of the third dimension to the face-on orbital profiles. Based on the models presented in Skokos, Patsis & Athanassoula (2002a,b, Papers I and II respectively), we investigate the parameters that favour the presence of boxy outer isophotes in the face-on profiles of 3D bars. As in most orbital structure studies, the models we present are not self-consistent. As underlined in Papers I and II, our goal is to study the orbital behaviour, and therefore the morphological changes, as a function of the model parameters. For this we consider even extreme cases, in order to make the effects clearest. We thus determine the main parameters that influence the boxiness of a model. We base our results not on the morphology of single orbits, but on collective appearance when orbits of more than one family are taken into account simultaneously. In parallel to this we study, as counterexamples, cases where the appearance of rectangular-like orbits close to the end of the bar are excluded. Finally, we discuss the correspondence between boxiness observed in edge-on profiles and boxiness observed in the middle of the bars when viewed face-on.

[2] We will hereafter refer to the Jacobi integral as the 'energy'.

2 FACE-ON PROFILES

In this series of papers (Papers I, II, and Patsis, Skokos & Athanassoula 2002, hereafter Paper III) we study the basic families in a general model composed of a Miyamoto disc of length-scales A = 3 and B = 1, a Plummer sphere bulge of scalelength 0.4 and a Ferrers bar of index 2 and axial ratio $a{:}b{:}c = 6 : 1.5 : 0.6$. The masses of the three components satisfy $G(M_{\rm D} + M_{\rm S} + M_{\rm B}) = 1$ and are given in Table 1. The length unit is 1 kpc, the time unit is 1 Myr and the mass unit is $2 \times 10^{11}\ {\rm M}_{\odot}$. In the present paper we examine two additional models. One of them, model B2, is characterized by a very strong bar, the mass of which is 40 per cent of the total, and whose remaining parameters are as in model B (Paper II). The other additional model has different axial ratios than the rest of our model bars. It has $a : b : c = 6 : 1 : 0.6$, instead of $a : b : c = 6 : 1.5 : 0.6$, as all others. It is used to study the contribution of families related to the radial 3 : 1 resonance to the appearance of boxy isophotes at the end of bars. The rest of its parameters are as in model A1, and we thus call it A1b. The basic properties of the models we present in this paper are summarized in Table 1.

A fundamental conclusion of Papers I and II is that essentially the backbone for building 3D bars is the x1 tree of families of periodic orbits. The tree consists of the x1 planar orbits and of its 3D bifurcations at the vertical resonances. Only in one case (family z3.1s in model B) did we find a family which supports the bar without being introduced in the system after a x1 bifurcation. In the

Table 1. Parameters of our models. G is the gravitational constant, $M_{\rm D}$, $M_{\rm B}$, $M_{\rm S}$ are the masses of the disc, the bar and the bulge respectively, $\epsilon_{\rm s}$ is the scalelength of the bulge, $\Omega_{\rm b}$ is the pattern speed of the bar, $R_{\rm c}$ is the corotation radius. The comment in the last column characterizes the model in order to facilitate its identification.

Model name	$GM_{\rm D}$	$GM_{\rm B}$	$GM_{\rm S}$	$\epsilon_{\rm s}$	$\Omega_{\rm b}$	$R_{\rm c}$	Comments
A1	0.82	0.1	0.08	0.4	0.0540	6.13	fiducial
A2	0.82	0.1	0.08	0.4	0.0200	13.24	slow bar
A3	0.82	0.1	0.08	0.4	0.0837	4.19	fast bar
B	0.90	0.1	0.00	–	0.0540	6.00	no bulge
C	0.82	0.1	0.08	1.0	0.0540	6.12	extended bulge
D	0.72	0.2	0.08	0.4	0.0540	6.31	strong bar
B2	0.60	0.4	0.00	–	0.0540	6.51	no bulge/very strong bar
A1b	0.82	0.1	0.08	0.4	0.0540	6.10	$a{:}b{:}c = 6{:}1{:}0.6$

present paper, we use these families in order to present the face-on views of the skeletons of the models. We use for this purpose sets of weighted orbits as in Paper III. As we explained in Paper III, in order to build a profile of weighted orbits for a model, we first calculate a set of periodic orbits and pick points along each orbit at equal time-steps. We keep only stable representatives of a family. The 'mean density' of each orbit (see Section 2.2 of Paper III) is considered as a first approximation of the orbit's importance and is used to weight the orbit. We construct an image (normalized by its total intensity) for each calculated and weighted orbit, and then, by combining sets of such orbits, we construct a weighted profile. The selected stable orbits are equally spaced in their mean radius. The step in mean radius is the same for all families in a model. We underline the fact that the orbital profiles we present throughout the paper comprise only stable periodic orbits.

As we have seen, the edge-on orbital profiles (Paper III) are of stair-type, which means that the families building the outer parts of the bars have the lowest $\overline{|z|}$. We are thus here mainly interested in orbits remaining close to the equatorial plane, since these orbits will contribute more to the surface density at the end of the bars.

2.1 Model A1

The fiducial case model A1 offers, also for the face-on structure of the models, a typical example of the contribution of the individual families to the observed face-on orbital morphology. Fig. 2 shows the weighted profiles of all contributing families. It is evident by simple inspection that the orbits of the 2D family x1 (Fig. 2a) are the most important, mainly because they have stable representatives over a large energy range. Nevertheless, the projections of the 3D families depicted from Fig. 2(c)–(h) play an important role. Contrarily, the x2 orbits (Fig. 2b) affect only the central parts of the system. As we can see, boxy features are related to the families x1v1 (Fig. 2c), x1v4 (Fig. 2e), x1v5 (Fig. 2f), x1v7 (Fig. 2g) and x1v9 (Fig. 2h). The family x1v3 (Fig. 2d), on the other hand, has always orbits with elliptical-like projections, thus in a way plays a complementary role, together with x1, providing building blocks for the elliptical-like part of the bar.

The orbits with the rectangular-like projections in model A1 face one of the main problems for explaining the boxy isophotes, i.e. they are less elongated than necessary. In general the boxy isophotes of the early-type bars are not squares. The rectangular-like orbits in model A1 also have shorter projections than the x1 ellipses on the semimajor axis. An exception is x1v9 (Fig. 2h). However, the four loops of these orbits are larger than can be admitted by the corresponding shapes of the isophotes of real galaxies. Furthermore, the x1v9 family contributes, because of its stability, only over a narrow energy interval ($-0.185 < E_j < -0.182$).

It is interesting to note that the boxy x1v1 orbits, responsible in many models for peanut-shaped edge-on profiles, give the face-on view of the system a 'bow-tie' structure. However, in this particular case at least, these orbits remain confined well inside corotation and can be responsible only for an inner boxiness in a galaxy and not for boxy isophotes at the end of the bars.

Fig. 3 combines all x1-related families, i.e. the 2D x1 family and its 3D bifurcations, as well as the x2 and the long-period banana-like orbits. We can see that the orbits support a bar with a semi-major axis of length about 0.75 of the corotation radius, so that the ratio of the corotation radius R_c to the orbital length of the bar a_o will be $R_c/a_o = 1.33$. The longest orbits along the bar are elliptical-like. This however, is not an obstacle to forming more rectangular-like bars, since the elliptical-like orbits extend only little beyond the rectangular-like ones. This extra extent could be suppressed if the outermost periodic elliptical-like orbits were not populated, or it could be masked by orbits trapped around the periodic rectangular-like ones. In the latter case, the isophotes (or rather isodensities) would be more elongated than the corresponding rectangular-like orbits.

We note that in a galaxy or in an N-body simulation, not all families included in the figure should be necessarily populated. In our non-self-consistent models we try to identify structures in order to seek their corresponding features in galactic images and snapshots of self-gravitating models.

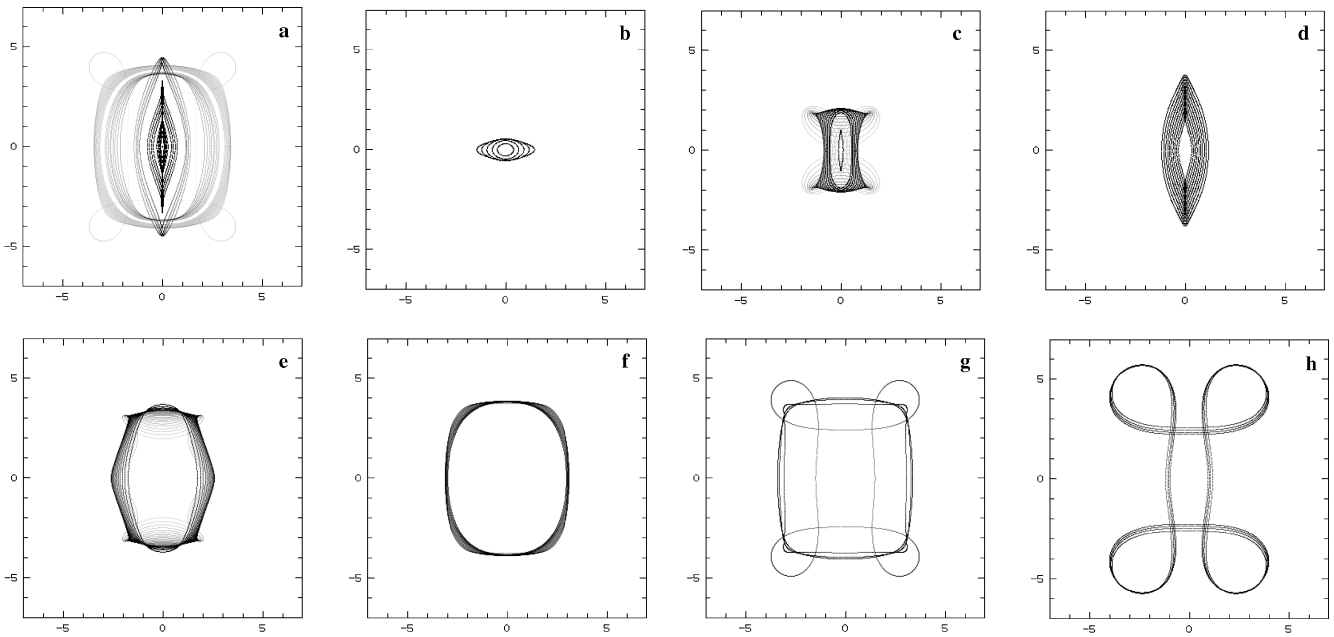

Figure 2. The face-on (x, y), weighted profiles of the 3D families in model A1. (a) x1, (b) x2, (c) x1v1, (d) x1v3, (e) x1v4, (f) x1v5, (g) x1v7, and (h) x1v9.

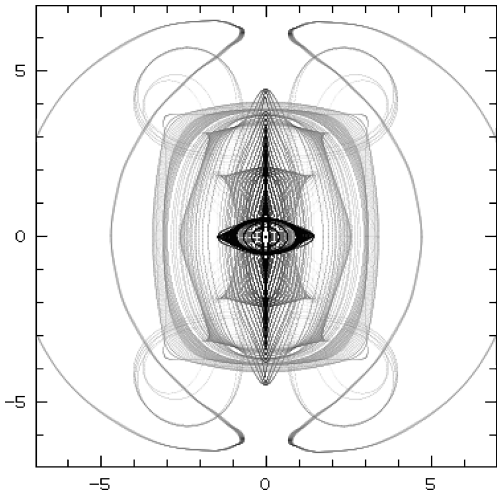

Figure 3. Face-on orbital profile for model A1. All x1-related orbits and the banana-like orbits are included, and they are weighted as described in Paper III.

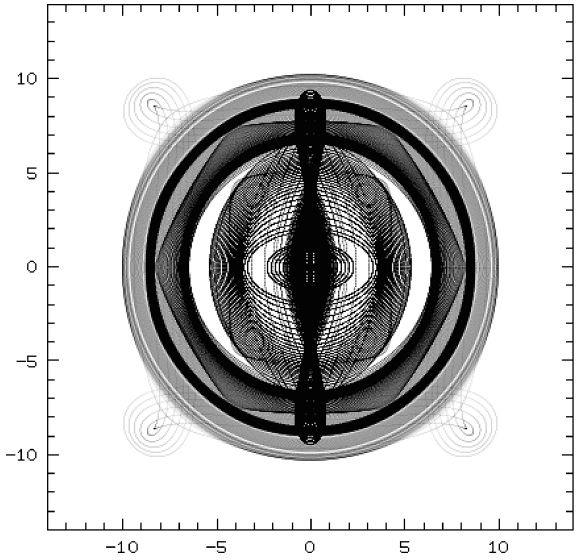

Figure 5. Face-on orbital profile for model A2. All orbits are weighted as described in Paper III.

2.2 Model A2

The slow rotating bar in model A2 brings new morphological features. In this case square- or rectangular-like orbits play a minor role, as we realize from Fig. 4. Only x1′ orbits (Fig. 4b) at the decreasing branch of the characteristic (Paper II) and part of the x1v1 family, after the S $\rightarrow$ Δ transition (Fig. 4c), provide such stable orbits to the system. For both these families, however, the size of the orbits and the energy range over which they exist do not allow them to play a major role in the orbital structure of the model. In Fig. 4b we choose the contrast of the image such as to allow us to see the loops of the x1′ square-like orbits. For even larger energies the loops of the x1′ square orbits become huge, and finally the orbits become retrograde. Such orbits are not depicted in Fig. 4(b).

Model A2 has two main features: First, the loops along the bar major axis, which are brought in the system by the x1 family and its x1v3 and x1v4 bifurcations. Second, the almost circular (and/or square-like) projections on the equatorial plane of the families x1′, x1′v4, and x1′v5 (Figs 4b, f and h respectively). The face-on morphology supported by this slow rotating bar is depicted in Fig. 5. In this figure we combine all orbits of the families presented in Fig. 4. The result is a bar with loops along the major axis surrounded by almost circular orbits. We note that the bar-supporting orbits extend to a distance about 9 from the centre (corotation in this case is at 13.24), i.e. in this case $R_c/a_o = 1.5$.

2.3 Model A3

If the bar rotates fast (model A3), the face-on orbital structure changes significantly. The x1 family dominates once again, as we can see in Fig. 6(a). Its orbits remain always elliptical-like, but now

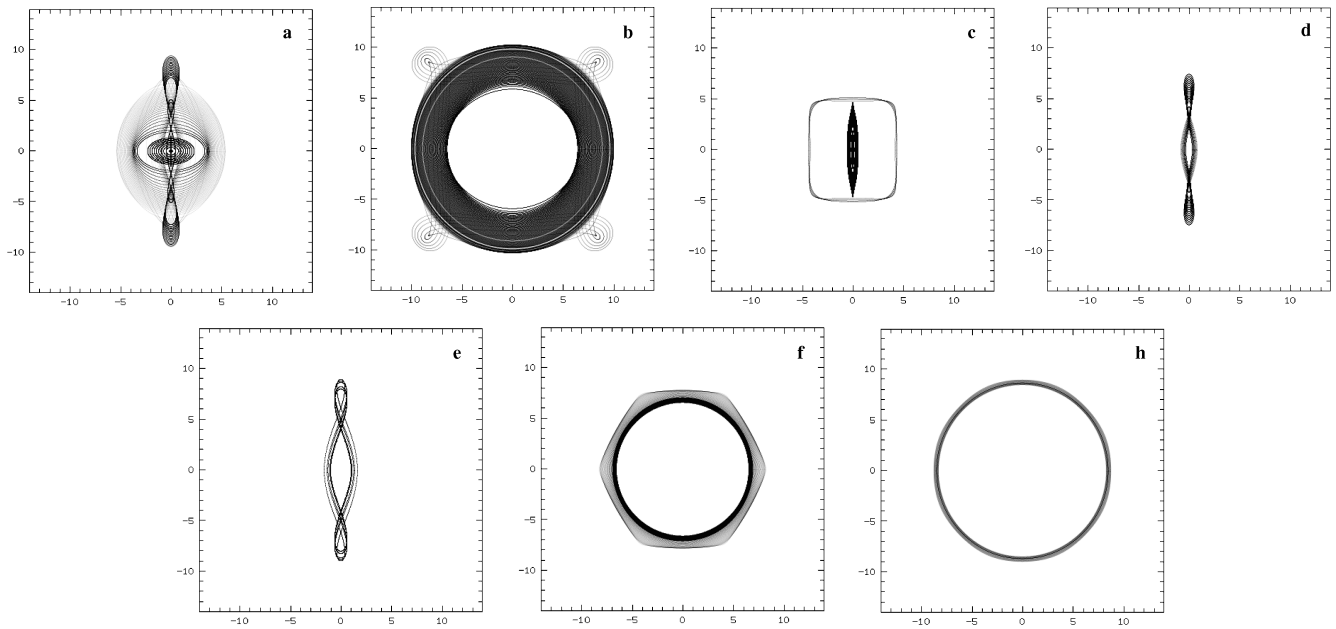

Figure 4. The face-on (x, y), profiles of the 3D families in model A2. (a) x1 and x2, (b) x1′, (c) x1v1, (d) x1v3, (e) x1v4, (f) x1′v4, and (h) x1′v5.

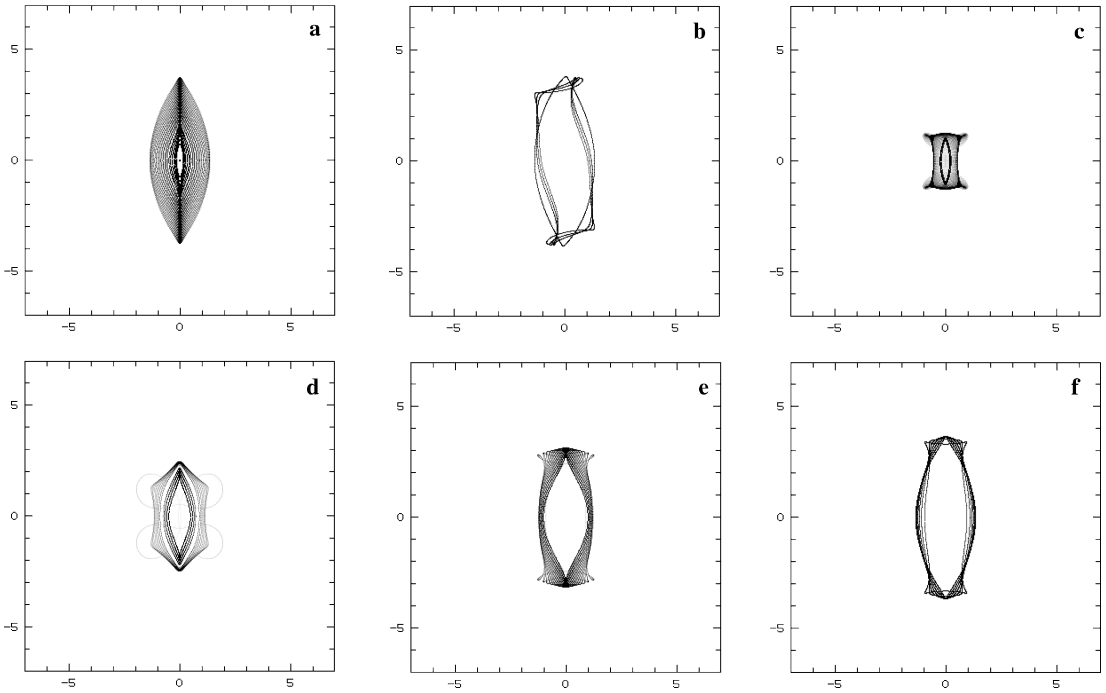

Figure 6. The face-on (x, y), profiles of the 3D families in model A3. (a) x1, (b) q0, (c) x1v1, (d) x1v3, (e) x1v5, (f) x1v8.

they support a bar with length 0.95 of the corotation radius, i.e. $R_c/a_o = 1.05$. The dynamics at the radial 4 : 1 resonance region are crucial for the morphology of the model (Paper II). In this case the families q0 and x1v8 provide the system with rectangular-like orbits quite elongated along the major axis of the bar. Family q0 can be found in two branches, symmetric with respect to the bar's major axis. We can, however, consider orbits of only one of its two branches if we want in our weighted profiles a non-rectangular parallelogram-like morphology. In order to obtain a desired morphology in our response models, we chose any combination of stable orbits from all available families. In the present case both families q0 and x1v8 have orbits at least as long as the x1 orbits. In addition, families x1v1 and x1v5 also have orbits with boxy projections on the equatorial plane, but reaching distances from the centre 1.2 and 3.2 respectively (Figs 6c and e). That means that, if all boxy families are populated, we can have boxy isophotes in several scales in this model. Even the hexagonal-like projections of the orbits of family x1v3 (Fig. 6d) contribute to the boxiness of the model with their sides that are parallel to the bar major axis. The face-on view of this family has also the 'bow-tie' appearance.

The total effect when considering all orbits is given in Fig. 7, where we take into account all families of Fig. 6. In Fig. 7(a) we give all weighted orbits together, while in Fig. 7(b) we apply a Gaussian filter in order to show clearly, in a first approximation, the shapes of features that could be supported by the orbits in the density maps of the models. Fig. 7 tells us that the fast rotating bar model has a boxy bar with $R_c/a_o \approx 1.05$.

The fast rotating bar case offers the opportunity to study models with a substantial non-axisymmetric force near corotation. In this way we compensate for the standard shortcoming of Ferrer's[3] ellipsoids, namely that their force drops too fast as the radius increases

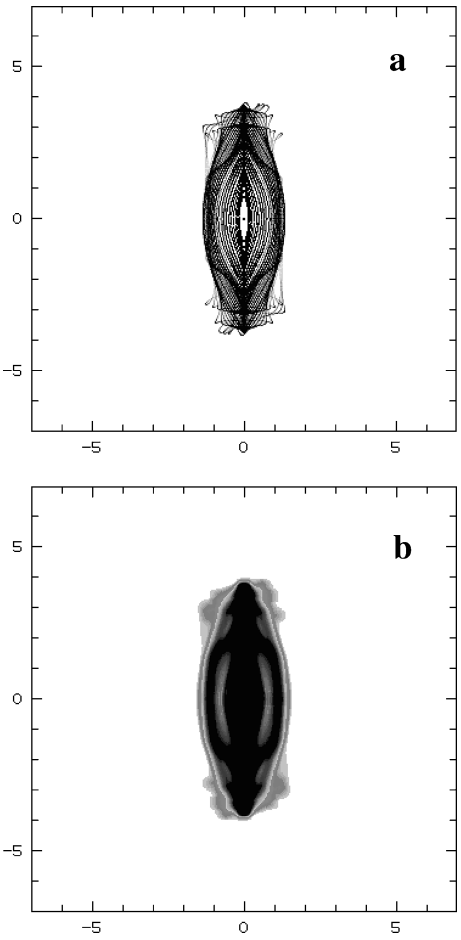

Figure 7. (a) Composite profiles combining all orbits in model A3. (b) The profile after applying a Gaussian filter in order to get an impression of the morphological features supported by the orbits.

[3] We use Ferrers bars because we are not aware of any other models which are *realistic* and *analytic*, and do not have this shortcoming.

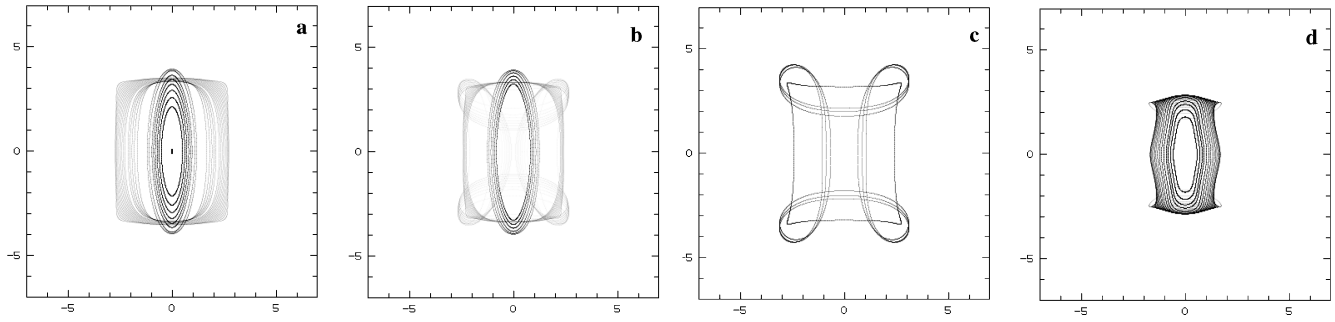

Figure 8. The face-on (x, y), profiles of the 3D families in model B. (a) x1, (b) x1v5 and x1v5′, (c) x1v7, (d) z3.1s.

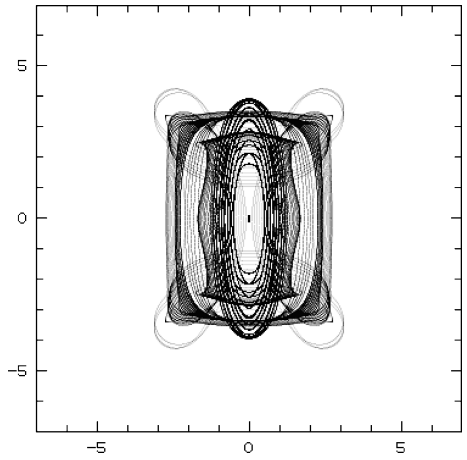

Figure 9. Composite profile combining the orbits of families x1, x1v5/x1v5′, x1v7 and z3.1s in model B.

and approaches corotation. Thus A3 allows us to cover also cases with substantial non-axisymmetric forcing near corotation.

2.4 Model B

Model B is a model without radial or vertical 2 : 1 resonances. As we have seen in Paper II, the first vertical bifurcation of x1 is x1v5. Thus, the families that build the bar are x1, x1v5/x1v5′, x1v7 and the family z3.1s. We remind the reader that this latter family plays a significant role in the orbital behaviour of this particular model (see Paper II) and it was found as a bifurcation of the z-axis orbits when the latter are considered as being of multiplicity 3, i.e. the orbits are repeated three times. The z3.1s family is not related to the x1-tree. The weighted face-on profiles of the above mentioned families are given in Fig. 8. We see that all of them have boxy representatives in their projections on the equatorial plane.

In Fig. 9 we have the orbital face-on view for model B obtained by overplotting the weighted orbits of all families together. In this model $R_c/a_o \approx 1.4$.

2.5 Model D

The strong bar model D is, after the fast rotating bar model A3, the second case where we have periodic orbits that can contribute to sufficiently elongated rectangular-like boxy isophotes. They are, however, considerably less elongated than the rectangular orbits in A3. As we see in Fig. 10, the main contributors are now families x1, x1v5/x1v5′ and x1v7. Again x1v1 orbits have 'bow-tie' face-on projections, and support a feature of corresponding morphology (Fig. 10b). This feature occupies the main part of the bar, but it does not reach its end, which is at about a distance 0.9 of the corotation radius.

The composite face-on orbital profile of model D is given in Fig. 11. We see that – although the boxy orbits are present and, if populated, could characterize the morphology of the model – the dominant feature is the loops of the x1 orbits along the major axis. This morphology is enhanced by the loops of the projections of the 3D bifurcations of x1, x1v5/x1v5′ and x1v6 (Fig. 10). It should be noted, however, that only the loops of x1v6 and some of the x1 loops extend beyond the rectangular outline. If we omit orbits with such loops we get, for this model, $R_c/a_o \approx 1.23$, while if we include them we get $R_c/a_o \approx 1.08$.

2.6 Very massive bars

In all the models we studied so far the rectangular-like orbits, if they exist, are rather square-like, except for the fast rotating bar case (model A3), where they are more elongated. The second parameter, after the pattern speed, which made the rectangular-like orbits more elongated is the increase of the relative mass of the bar. For this reason, we studied several more models with increased bar mass fraction and calculated the orbital stability of each individual case. We stopped when we reached models with very large intervals of instability of the x1 family and its 3D bifurcations. From a sequence of models starting with the values of the parameters of model B and with an increasingly large fraction of mass in the bar, we found that this fraction is about 50 per cent of the total mass. It was evident that models with bar masses about 40 per cent of the total mass offered families of periodic orbits with enough stable representatives to support sufficiently elongated rectangular-like isophotes at the end of the bars. For example, model B2, which differs from model B only in that the mass of the bar $GM_B = 0.4$ instead of 0.1 as in model B, has rectangular-like orbits with the ratio of their projections on the major axis of the bar to their projections on the minor axis (p_{max}/p_{min}) close to 2. This can be seen in Fig. 12. In Fig. 12(a) we have orbits from the families x1, x1v5/x1v5′ and x1v7, omitting rectangular-like orbits with loops. The blurred image in Fig. 12(b) includes also orbits of the t1 family (see Paper I) and stable orbits of family x1v6. The latter is initially bifurcated as unstable. For larger energies, however, it has stable orbits with face-on projections with loops along the major axis of the bar. The t1 orbits, bifurcated at the radial 3 : 1 resonance, introduce in the system some interesting features if one considers both their branches which are symmetric with respect to the minor axis of the bar at a given energy. The t1 orbits are responsible for the guitar-like feature we observe in

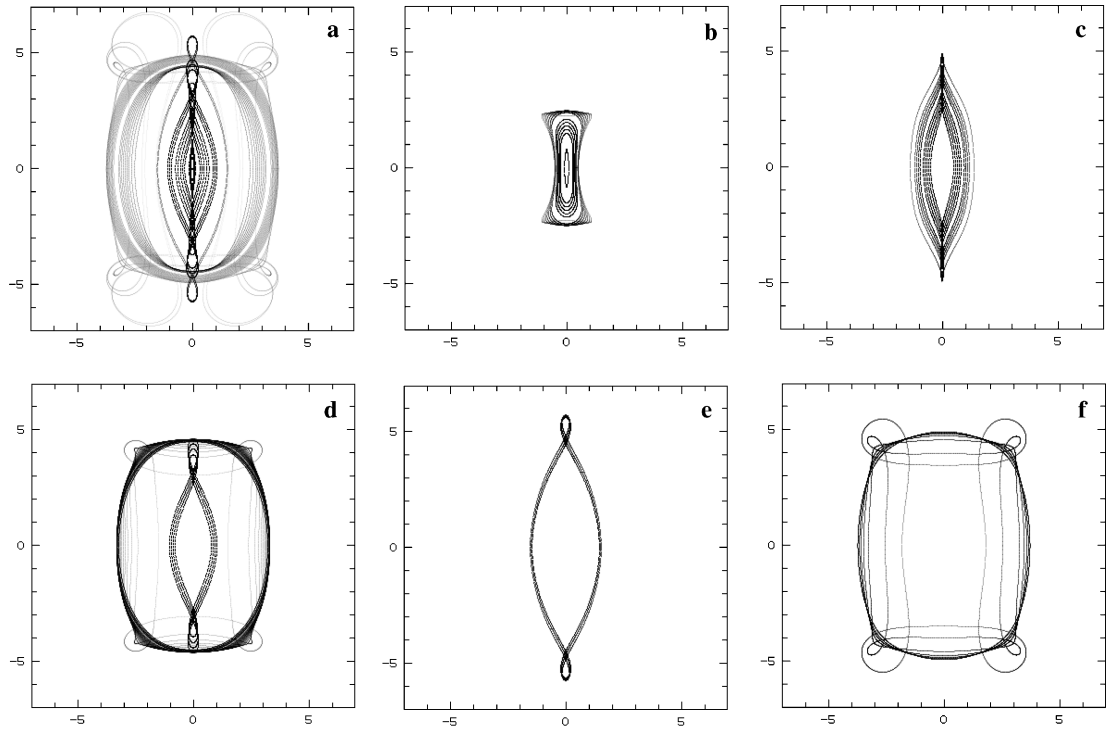

Figure 10. The face-on (x, y), profiles of the 3D families in model D. (a) x1, (b) x1v1, (c) x1v3, (d) x1v5/x1v5′, (e) x1v6, (f) x1v7.

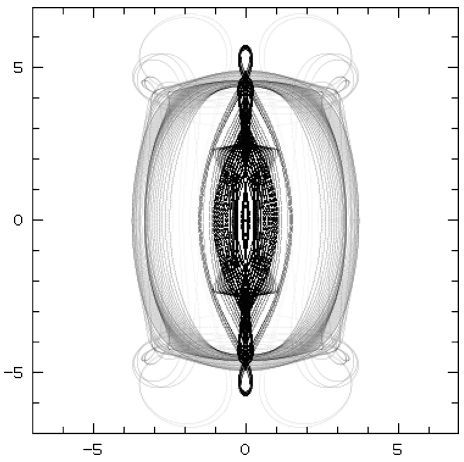

Figure 11. Composite face-on profile of model D. All orbits of Fig. 10 are considered.

Fig. 12(b) closer to the major axis than the outer rectangular-like orbits. For model B2 we have $R_c/a_o \approx 1.04$.

2.7 Support by 3 : 1 families

The contribution of t1 to the features we found in model B2 gave us the incentive to investigate the contribution of families bifurcated at the radial 3 : 1 resonance in all our models. We found that in general orbits from the t1 family may support motion roughly parallel to the minor axis of the bar, but not at the end of the bar. Fig. 12(b) describes the kind of contribution t1 orbits can offer to the overall boxiness of face-on profiles of barred galaxies. We give also an example of the combination of t2 orbits (see Paper I) in a model in which this contribution is pronounced. It is model A1b, a model that differs from the fiducial case (model A1, Paper I) only in the axial ratios, which in model A1b are $a : b : c = 6 : 1 : 0.6$ instead of $a : b : c = 6 : 1.5 : 0.6$. In Fig. 13 we observe stable x1 orbits with loops along the major axis of the bar, and x1 orbits with a more or less rectangular like shape. The two groups are separated by an empty region caused by an instability region of the x1 family. On top of the x1 orbits we overplot stable orbits of both branches, symmetric with respect to the major axis of the bar, of the t2 family. The t2 orbits contribute to the boxiness of the model by enhancing the borders of the empty region and by forming a rectangular-like feature indicated in Fig. 13 by four black arrows. Model A1b has $R_c/a_o \approx 1.35$.

3 DISCUSSION

We examined the face-on views of all models of Papers I and II and we found families that could support outer, as well as inner, boxy isophotes. In the present paper we do not refer explicitly to model C, since its orbital behaviour does not differ essentially from that of model A1. Furthermore, we use composite profiles of two additional models to demonstrate the effect of very massive barred components and the possible role of families related to the radial 3 : 1 resonance.

The first quantity that can be used to compare the bars of our models with the bars of real galaxies concerns the length of the bar built by the orbits with respect to corotation radius. Indeed observations (for a compilation see e.g. Athanassoula 1992b; Elmegreen 1996; Gerssen 2002) as well as hydrodynamical simulations (Athanassoula 1992b), have shown that the ratio R_c/a_o takes values only in a restricted range, namely $R_c/a_o = 1.2 \pm 0.2$. This is in agreement with 2D orbital models by Contopoulos (Contopoulos 1980). All our response models have R_c/a_o ratios within this range, except for model A2 which has a slow rotating bar and $R_c/a_o = 1.5$.

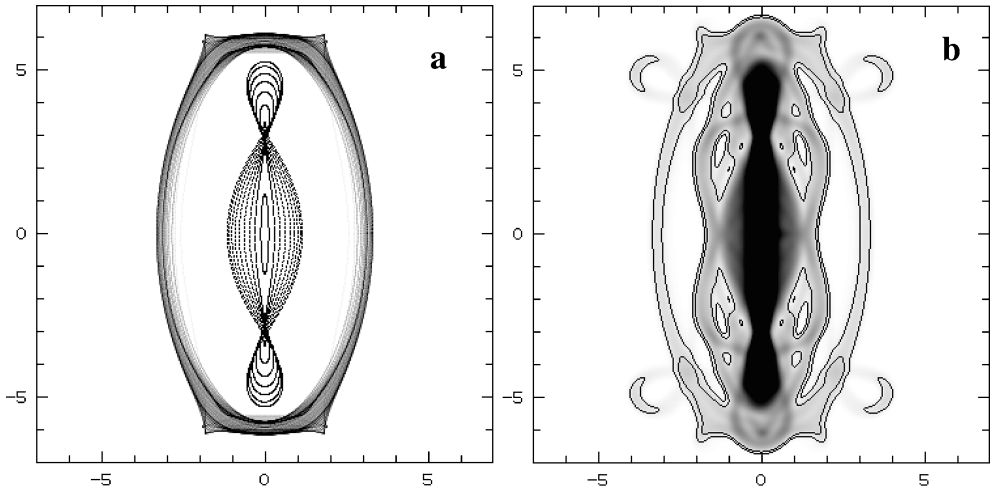

Figure 12. (a) A composite face-on profile of model B2. We consider orbits from the families x1, x1v5/x1v5′and x1v7. (b) The blurred profile of model B2. Besides the x1, x1v5/x1v5′ and x1v7, we consider stable orbits of x1v6 and 2D orbits of family t1. In model B2 we can have rectangular-like face-on profiles with $p_{\max}/p_{\min}$ ratio close to 2.

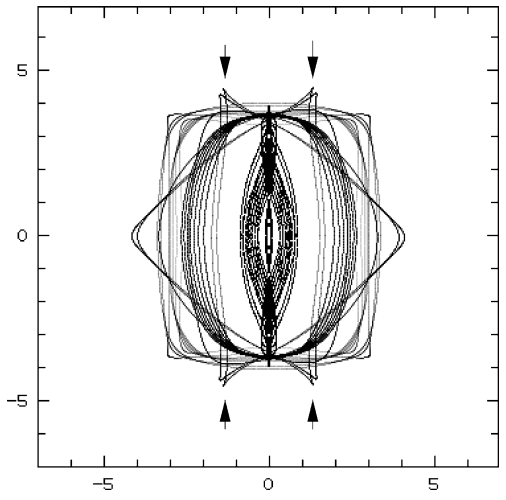

Figure 13. x1 and t2 orbits in model A1b. The elliptical-like orbits with loops along the major axis of the bar are clearly separated from the rest of the orbits. Owing to orbital instabilities the boundary between the two regions has a rectangular-like shape and is enhanced by the t2 orbits. Its four corners are indicated by arrows.

Table 2 summarizes the R_c/a_o ratios for the models we studied in the present paper.

A second quantity we can compare with galaxies and snapshots of N-body models is the ratio $p_{\max}/p_{\min}$ for the rectangular-like orbits. Eye estimates show that the boxy outer isophotes at the end of the bar of strongly barred galaxies have a ratio $p_{\max}/p_{\min}$ typically larger than 2 (e.g. NGC 936, NGC 4314, NGC 4596). Exceptional cases can be found in the literature but are not many (see e.g. the not-rectified images of NGC 1415 in Garcia-Barreto & Moreno (2000)). A more quantitative study has been made by Athanassoula et al. (1990). They find that the axial ratios of the isophotes near the end of the bar are, for all the galaxies in their early-type strongly-barred galaxy sample, considerably larger than 2. On the other hand, in most of our models the boxy orbits are quite square-like. Ratios of boxy isophotes larger than 2 have been mainly found in the fast rotating bar case, where $p_{\max}/p_{\min} \approx 2.5$. The strong bar model D has $p_{\max}/p_{\min} \approx 1.4$, while in model B2, where the mass of the bar is 40 per cent of the total mass, we attained a $p_{\max}/p_{\min}$ ratio close to 2. In the rest of the models the ratio was less than 1.4.

Table 2. The ratio of the corotation radius R_c to the orbital length of the bar a_o (R_c/a_o) for all models studied in the present paper. We find $1.04 \leqq R_c/a_o \leqq 1.5$. The third column gives a short comment about what characterizes the model in order to facilitate its identification.

Model name	R_c/a_o	Comments
A1	1.33	fiducial
A2	1.50	slow bar
A3	1.05	fast bar
B	1.40	no bulge
D	1.08	strong bar
B2	1.04	no bulge/very strong bar
A1b	1.35	$a:b:c = 6:1:0.6$

Let us underline that, for studying the elongation of the rectangular-like isophotes observed in barred galaxies, one needs to combine orbits of several families instead of evaluating the properties of a single orbit or a single family. This is a result of the 3D character of our models and of the fact that we have bars built by orbits belonging mainly to the x1 tree. This effect is indicated by isodensities we plotted on some blurred images of our models. Such a typical case is given in Fig. 14, for model B. The small sides of the rectangular-like structure outlined by the isophotes reflect mainly the contribution of the rectangular-like orbits. However, the two large sides, parallel to the major axis of the bar, are due to the overlapping of orbits of the x1 and z3.1s families.

Our models show that it is the pattern speed that mainly determines the elongation of the outer boxy orbits. The orbits building the bar of model A3 are rectangular-like and could make a bar with the geometry encountered in the early-type bars with outer boxy isophotes. It is just the increase of Ω_b that brought in the system the 2D family q0 and the 3D, stable x1v8 orbits. We note the morphological similarity of the q0 orbits with the outer boxy isophotes of NGC 4314 (Quillen, Frogel & Gonzalez 1994), which have the form of a non-rectangular parallelogram (compare Fig. 7b with Fig. 1).

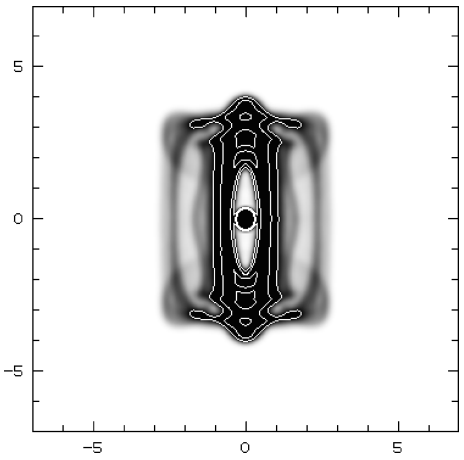

Figure 14. Isodensities on a blurred image of model B. The narrow rectangular-like structure is supported by orbits of more than one family.

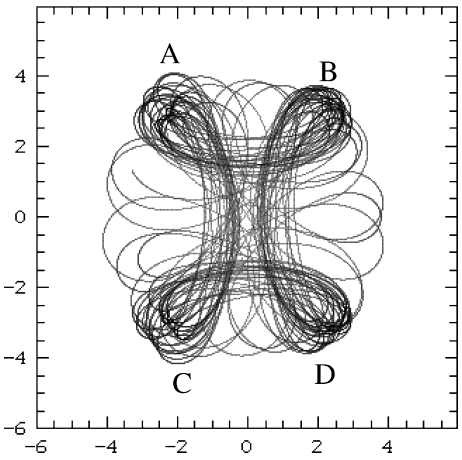

Figure 15. An example of a chaotic orbit in Model B, that, for a small number of dynamical times, supports a 'bow-tie' morphology. A particle following this trajectory spends most of the time in the regions of the loops indicated with A, B, C and D, while the 'arcs' $\widehat{AC}$ and $\widehat{BD}$ approach the centre of the galaxy. Darker areas indicate regions where the orbit spends more time.

We note that in model A3 the rectangular-like bar ends closer to corotation than the bars of the models for which the longest orbits are the x1 with loops along the major axis. This is consistent with the result found in Patsis et al. (1997a) for the pattern speed of NGC 4314, in which the boxy isophotes are very close to the corotation radius indeed. It is also obvious that, apart from the increase of the pattern speed, the increase of the strength of the bar favoured the elongation of the rectangular-like orbits.

Model A2, which is the slowest rotating case, is the other extreme of the face-on morphologies we encounter in our models. In this model, planar boxy orbits and projections of orbits on the equatorial plane are square-like, and very little elongated along the major axis of the bar (Fig. 4c of the present paper, and fig. 5 in Paper II). The development of loops at the apocentra of the x1 elliptical-like orbits, as well as in the projections on the equatorial plane of the x1v3 and x1v4 families, together with the almost circular x1′ orbits and the projections of the x1′v4 and x1′v5 families, give to model A2 a characteristic face-on morphology with the circular-like orbits surrounding all other orbits in the face-on projection. Such a morphology could be linked to the existence of inner rings in barred galaxies.

Inner boxiness of the face-on profiles, much closer to the centre than the corotation region, is associated mainly with the x1v1 orbits, i.e. with the 3D family born at the vertical 2 : 1 resonance. As we have seen in Paper III, in several models this family is responsible for peanut-shaped orbital structures in the edge-on views of the models. The face-on orbital skeletons of the models we present here show in another clear way what we noticed in Paper III, namely that the x1v1 family builds boxy- or peanut-shaped features which do not approach corotation. Inner boxiness is not rare in galactic bars. Typical examples of boxy isophotes in the middle of the stellar bars are NGC 3992 and NGC 7479 (Wilke, Möllenhoff & Matthias 2000). The x1v1 orbits, or at least their representatives with the largest energy values (see Figs 2c, 6c and 10b), are boxy in their face-on views, but they also have a characteristic 'bow-tie' morphology. Inner boxiness is also supported by the z3.1s orbits, at large values of the energy, in model B.

A 'bow-tie' morphology in models of the kind we study here can also be introduced by rectangular-like orbits at high energies. These orbits (or more precisely their face-on projections) develop loops, which, in some cases, stay close to the orbits that build the bulk of the bar. This is e.g. the case for the x1v5′ family in model B (Fig. 8b). When the rectangular-like orbits develop loops they also become of 'bow-tie' shape. Since their deviations from the equatorial plane increase with energy, their projections occupy almost the same area as the rectangular-like orbits of the same family, for lower energies, do. In model B, for $E_J \approx -0.185$, integrating even chaotic orbits for a *small* number of dynamical times (of the order of 30) we obtain a bow-tie morphology. This is shown in Fig. 15. Non-periodic elliptical-like orbits trapped around the x1 family not far from the centre of the bar, as well as the projection of orbits trapped around the 3D x1 bifurcations, would fill more densely the area between the regions A and B (and symmetrically between C and D) than that between the regions A and C (and B and D). This results from the elliptical-like shape of the projections of these orbits on the equatorial plane and the fact that they have their apocentres between the regions A and B (and C and D). We note also the contribution of the x1v1 orbits to a 'bow-tie' morphology of face-on profiles, as mentioned previously.

Owing to the presence of these families, a bow-tie morphology, like the one found by Barnes & Tohline (2001), is not excluded from the usual barred morphology. Nevertheless, we did not find orbits of a single family that can enhance simultaneously both a rectangular-like structure at the end of the bar without loops at its four corners and a bow-tie morphology. Single families with bow-tie profiles in their face-on projections do not extend to the end of the bar (x1v1 in Figs 2c, 6c, 10b and x1v3 in Fig. 6d).

4 CONCLUSIONS

In this paper we discussed boxiness in the face-on views of 3D models, and, in general, their face-on orbital structure. We examined a large variety of possible 3D orbital behaviour that could contribute to the boxiness in face-on views of barred galaxies. Our main conclusions are as follows.

(i) Boxiness in the face-on views of 3D barred models is an effect caused by the coexistence of several families, each contributing appropriate stable orbits. The morphology of boxy isodensities/isophotes is not necessarily similar to the morphology of

individual stable, rectangular-like orbits. In some cases (Fig. 14) the isocontours can be narrower than the orbits.

(ii) In models with the right morphological parameters, we find appropriate building blocks to account for the rectangular-like isophotes or isodensities seen in early-type barred galaxies and in some *N*-body simulations.

(iii) In 3D models the family of the planar x1 orbits is subject to vertical instabilities, and thus in several cases it has significant instability strips at the 4 : 1 resonance region. This should be an obstacle in using x1 planar orbits to account for the rectangular-like shape of bars, since unstable periodic orbits can not trap regular orbits around them. However, at the instability regions of the x1 we find other stable families, the (x, y)-projected orbital shapes of which are, at least near their bifurcations, very similar to those of the x1. They have orbits that are stable over large energy intervals and also have (x, y)-projected shapes that can enhance a rectangular-like bar outline. Thus the inclusion of the third dimension in the models enhances the possibility of rectangular-like isodensities.

(iv) There are families of periodic orbits that support boxiness in the outer bar regions, as well as families that support boxiness in somewhat more inner parts. The standard families belonging to the former category are the stable representatives of the x1 orbits (close to the radial 4 : 1 resonance), and of the families x1v5, x1v7 and x1v9. The families q0 and x1v8 play a major role in model A3 and thus could be essential for fast rotating bars. Nevertheless, the geometry of a boxy feature becomes evident mainly in weighted profiles, where orbits from one or more families are considered. Inner boxiness is associated mainly with the x1v1 family and, in model B, with family z3.1s.

(v) Orbits of the families related to the 3 : 1 resonance (t1 and t2) may contribute in some cases to the boxiness of the profiles. The t1 family can do this by supporting motion parallel to the minor axis of the bar at intermediate distances between the galaxy centre and corotation, and the t2 family by enhancing the sides of the boxes parallel to the major axis.

(vi) The consideration of several families of orbits for building a profile may lead to boxy features close to the end of bars, with $p_{\max}/p_{\min}$ ratios different from the corresponding ratios of individual orbits or families of orbits.

(vii) An essential conclusion of our investigation is that outer boxiness is favoured by fast bar pattern speeds, while in the slow-rotating model the bar is surrounded by almost circular orbits. These are the two extremes of an orbital behaviour that changes as the pattern speed varies from one model to the other. The near-circular orbits could be building blocks for inner rings.

(viii) The fast rotating bar has a length 0.95 of its corotation radius, while the slow one only 0.68. This indicates that boxy bars end close to their corotation, while the end in slow rotating bars might be associated with $n : 1$ resonances of lower n values.

(ix) The rectangular-like orbits in models with faster bars are more elongated than the corresponding orbits in models with slower bars. When modelling individual barred galaxies, for which we know a priori that in general $1 < R_c/a_o < 1.4$, the elongation of the orbits can be used to give estimates of, or at least set limits to, the bar pattern speed, without the use of kinematics, which is not always available.

(x) The second most efficient way of stretching rectangular-like orbits is to increase the mass of the bar. This mechanism, however, is restricted by the fact that in very strong bars the families of periodic orbits which support the boxy face-on profiles are unstable over large energy intervals.

(xi) Outer boxy, 'bow-tie' morphology is possible in some models by combining orbits of several families. A necessary condition for this is to have 4 : 1 type orbits with loops close to the main bar. Inner 'bow-tie' morphology can be due to the presence of x1v1 orbits (Figs 2c, 6c and 10b).

ACKNOWLEDGMENTS

We acknowledge fruitful discussions with and very useful comments by G. Contopoulos and A. Bosma. We thank the anonymous referee for valuable remarks, which improved the paper. This work has been supported by ΕΠΕΤ II and ΚΠΣ 1994–1999 and by the Research Committee of the Academy of Athens. ChS and PAP thank the Laboratoire d'Astrophysique de Marseille for an invitation during which essential parts of this work have been completed. ChS was partially supported by the 'Karatheodory' post-doctoral fellowship No. 2794 of the University of Patras. All image processing work has been done with ESO-MIDAS. DSS was produced at STSI under US Government grant NAG W-2166. The images of these surveys are based on photographic data obtained using the Oschin Schmidt Telescope on Palomar Mountain and the UK Schmidt Telescope.

REFERENCES

Athanassoula E., 1984, Phys. Rep., 114, 319
Athanassoula E., 1992a, MNRAS, 259, 328
Athanassoula E., 1992b, MNRAS, 259, 354
Athanassoula E., Misiriotis A., 2002, MNRAS, 330, 35
Athanassoula E., Bienaymé O., Martinet L., Pfenniger D., 1983, A&A, 127, 349
Athanassoula E., Morin S., Wozniak H., Puy D., Pierce M. P., Lombard J., Bosma A., 1990, MNRAS, 245, 130
Barnes E. J., Tohline J. E., 2001, ApJ, 551, 80
Buta R., 1986, ApJS, 61, 631
Contopoulos G., 1980, A&A, 81, 198
Contopoulos G., 1988, A&A, 201, 44
Contopoulos G., Grosbøl P., 1989, A&AR, 1, 261
Debattista V. P., Sellwood J. A., 2000, ApJ, 543, 704
Elmegreen D., 1996, in Buta R., Crocker D., Elmegreen B., eds, ASP Conf. Ser. Vol. 91, Barred galaxies. Astron. Soc. Pac., San Francisco, p. 23
Friedli D., Benz W., 1993, A&A, 268, 65
Garcia-Barreto J. A., Moreno E., 2000, ApJ, 529, 832
Gerssen J., 2002, in Athanassoula E., Bosma A., Mujica R., eds, ASP Conf. Ser. Vol. 275, Disks of Galaxies, Kinematics, Dynamics and Perturbations. Astron. Soc. Pac., San Francisco, p. 197
Ohta K., Hamabe M., Wakamatsu K., 1990, ApJ, 357, 71
Patsis P. A., Athanassoula E., Quillen A. C., 1997a, ApJ, 483, 731
Patsis P. A., Efthymiopoulos C., Contopoulos G., Voglis N., 1997b, A&A, 326, 493
Patsis P. A., Skokos Ch., Athanassoula E., 2002, MNRAS, 337, 578 (Paper III)
Pfenniger D., 1984, A&A, 134, 373
Pfenniger D., 1985, A&A, 150, 112
Quillen A. C., Frogel J. A., Gonzalez R. A., 1994, ApJ, 437, 162
Shaw M., Combes F., Axon D. J., Wright G. S., 1993, A&A, 273, 31
Skokos Ch., Patsis P. A., Athanassoula E., 2002a, MNRAS, 333, 847 (Paper I)
Skokos Ch., Patsis P. A., Athanassoula E., 2002b, MNRAS, 333, 861 (Paper II)
Wilke K., Möllenhoff C., Matthias M., 2000, A&A, 361, 507

This paper has been typeset from a TEX/LATEX file prepared by the author.